



Tight Focusing of a higher order Radially Polarized sinh-Gaussian beam Transmitting through Cosine Phase Plate

R. Vijay Kumar, K. Prabakaran, K.B. Rajesh, A. Mohamed Musthafa, V. Aroulmoji

► To cite this version:

R. Vijay Kumar, K. Prabakaran, K.B. Rajesh, A. Mohamed Musthafa, V. Aroulmoji. Tight Focusing of a higher order Radially Polarized sinh-Gaussian beam Transmitting through Cosine Phase Plate. International journal of advanced Science and Engineering, 2023, 10 (1), pp.3329-3335. <10.29294/IJASE.10.1.2023.3329-3335>. <hal-04194672>

HAL Id: hal-04194672

<https://hal.science/hal-04194672v1>

Submitted on 4 Sep 2023

HAL is a multi-disciplinary open access archive for the deposit and dissemination of scientific research documents, whether they are published or not. The documents may come from teaching and research institutions in France or abroad, or from public or private research centers.

L'archive ouverte pluridisciplinaire **HAL**, est destinée au dépôt et à la diffusion de documents scientifiques de niveau recherche, publiés ou non, émanant des établissements d'enseignement et de recherche français ou étrangers, des laboratoires publics ou privés.



HAL Authorization

Tight Focusing of a higher order Radially Polarized sinh-Gaussian beam Transmitting through Cosine Phase Plate

R.Vijay Kumar¹, K.Prabakaran^{1*}, K.B.Rajesh², A. Mohamed Musthafa³, V.Aroulmoji⁴

¹Department of Physics, Mahendra Arts and Science College (Autonomous),
Namakkal, Tamilnadu, India

²Department of Physics, Chikkanna Government Arts College, Trippur, Tamilnadu, India

³Department of General Studies (Physics Group), Jubail University College (Male Branch),
Royal Commission of Jubail, Kingdom of Saudi Arabia

⁴Center for Research and Development, Mahendra Engineering College, (Autonomous),
Mallasamudram-637503, Tamilnadu, India

ABSTRACT: The tight focusing of a double ring-shaped radially polarized sinh-Gaussian beam with a cosine phase plate is studied on the basis of the vector diffraction theory. Under a high-NA focusing condition, the strong longitudinal component forms a sharper spot at the focal point for both fundamental mode (R-TEM₀₁*) beams and higher-order, radially polarized mode beams. Due to destructive interference between the inner and outer rings, double-ring-shaped radially polarized mode (R-TEM₁₁*) beams in particular can significantly lower the focal spot size. Simulation results show that the focused fields and phase distributions at focus are largely influenced by both the cosine parameter and truncation coefficient of the incident beams. Moreover, shifted focal spot, optical cage patterns can be flexibly achieved by carefully choosing the cosine parameter (C) and it is also observed that the intensity distribution of the different mode has little variation among the degree of truncation (β) of the input beam beside the pupil. This work is important for optical manipulation, particle limitation systems, laser surface modification and laser direct writing techniques.

KEYWORDS: Higher order Sinh Gaussian beam, Vector diffraction theory, High NA lens, cosine phase plate.

<https://doi.org/10.29294/IJASE.10.1.2023.3329-3335> ©2023 Mahendrapublications.com, All rights reserved

INTRODUCTION

A single-ring-shaped radially polarized beam, which is often referred to as an R-TEM₀₁* mode beam, is of particular interest. In the case of high-numerical-aperture (NA) focusing the R-TEM₀₁* beam can generate a strong longitudinal electric field at the focus [1]. This strong longitudinal component creates a tight focus that may increase the resolution of microscopes [2,3] and improve laser cutting capabilities in processing materials [4]. Numerous techniques for producing the radially polarized beam have been described due to the benefits of the beam that were previously discussed. Zhan [5] discovered that the scattering force along the optical axis is zero in 2004, when he estimated the radiation forces on metallic Rayleigh particles at the focus using a highly focused vector R-TEM₀₁* beam. This performance is highly helpful in capturing metallic particles that absorb metal. Due to the

decreased scattering, Kawauchi et al., [6] and Nieminen et al., [7] showed that R-TEM₀₁* beams can be utilized to enhance the functionality of optical tweezers in the geometrical optics domain and the Mie regime. Yan and Yao [8] demonstrated, the radiation forces on more general dielectric particles with size ranging from the Rayleigh regime to several wavelengths, illuminated by a highly focused R-TEM₀₁* beam. Ahluwalia et al., [9] reported experimentally the polarization-induced torque of an R-TEM₀₁* beam acting on anisotropic micro-particles.

The R-TEM₀₁* beam is superior to the linearly polarized beam in the Rayleigh domain, according to the analytical studies reported by Chen et al., [10]. A doughnut-shaped (single-ring) radially polarized beam was produced by superimposing the two orthogonally polarized Gaussian modes TEM₁₀ and TEM₀₁ outside or

*Corresponding Author: prabakaran27mar@gmail.com

Received: 20.06.2023

Accepted: 17.07.2023

Published on: 25.08.2023

Vijay Kumar et al.,

within a laser cavity [11,12]. Recently, Kozawa et al., reported that the radially polarized higher-order Laguerre-Gaussian beam (LG) has higher performance than the low-order one and can generate the focal spot beyond the Abbe's diffraction limit 0.5λ [13-15]. Tian and Pu [16] also utilized the double-ring-shaped azimuthally polarized LG beam to form a sub wavelength focal hole near the focus. Recently, it was experimentally detected directly on or after a laser cavity by a higher order radially polarized mode R-TEM₁₁* [17]. Moreover, these high frequencies can be radially polarized through special cavities designed for oscillation. It has also been reported that two radially polarized circles can create a dark field around the focal point under high velocity conditions [18]. This kind of higher-order LG beam has concentric multi ring-shaped intensity pattern with π phase shift between the rings.

Focal shifts are crucial for image creation in defocused planes, for improving the depth of field, and for automatic focusing [19]. They have also been played a significant role in the design and optimization of many optical systems. More intriguingly, in some optical focusing systems, the focal shift may be continuous. It was discovered that the focus switch a phenomenon known as an effective permutation of the focal point could occur along with the focal shift. It

was found that the point of absolute maximum intensity does not coincide with the geometrical focus but shifts along the optical axis. This phenomenon is called focus shift. More intriguingly, in some optical focusing systems, the focal shift may be continuous. It would be quite fascinating to look at the focusing characteristics of this form of radially polarized light beam since this could help us better understand its characteristics and broaden the range of possible applications. In this article, we examine the focusing properties of a higher-order radially polarized sinh Gaussian beam with a cosine phase plate.

2. Vector diffraction theory

Figure 1 displays a schematic diagram of the proposed technique. The higher order radially polarized sinh Gaussian beam with cosine phase plate and then focused through a high NA lens system. The research was carried out using the widely utilized high-NA lens system at arbitrary incident polarization vectorial diffraction method of Richards and Wolf [20]. The electric field $E(r,z)$ at the focus region can be expressed as using the cylindrical coordinates r, z , and the notations from Ref. [1]. the electric field $E(r,z,\phi)$ in the vicinity of the focal region can be written as:

$$\vec{E}(r, z) = E_r \vec{e}_r + E_z \vec{e}_z \rightarrow (1)$$

Where E_r and E_z are the amplitudes of the two orthogonal components \vec{e}_r, \vec{e}_z are their corresponding unit vectors. The electric field's two orthogonal components are represented as

$$E_r(r, z) = A \int_0^\alpha \sqrt{\cos(\theta)} \sin 2\theta P(\theta) l(\theta) J_1(kr \sin \theta) e^{ikz \cos \theta} d\theta \rightarrow (2)$$

$$E_z(r, z) = 2iA \int_0^\alpha \sqrt{\cos(\theta)} \sin^2 \theta P(\theta) l(\theta) J_0(kr \sin \theta) e^{ikz \cos \theta} d\theta \rightarrow (3)$$

Where $\alpha = \arcsin(NA)/n$ the maximal angle is determined by the numerical aperture of the objective lens

And n is the index of refraction between the lens and the sample. $k = 2\pi/\lambda$ is the wave number and $J_n(x)$ is the Bessel function of the first kind with order n . r and z are the radial and z coordinates of observation point in focal region, respectively. $P(\theta)=1$ describes the pupil

apodization function. The intensity in the focal region is proportional to the square modulus of Eq. (1). The wavefront phase distribution in the system examined in this article is a radial cosine function distribution, and it may be represented as [21]

$$\phi = \pi \cdot \cos \left[\pi \cdot C \frac{\tan(\theta)}{\tan(\alpha)} \right] \rightarrow (4)$$

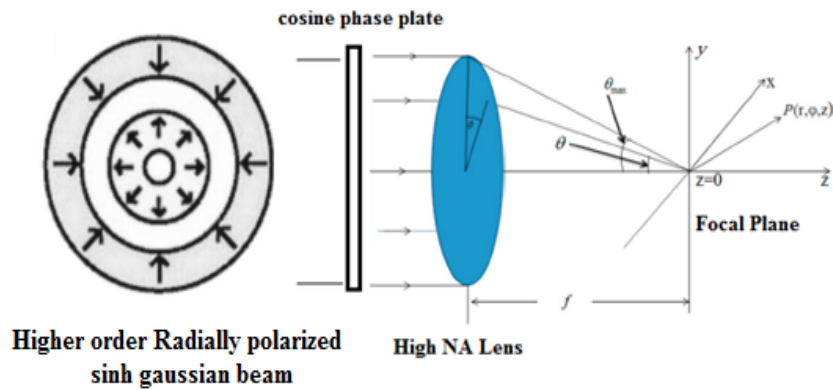


Fig 1: Focusing of a radially polarized sinusoidal Gaussian beam with a radial cosine phase plate through a high numerical aperture lens

Where C is the frequency parameter in the wavefront phase distribution's cosine component. This type of radial cosine phase wavefront was chosen because it is relatively straightforward and easy to construct. For instance, this type of phase distribution can be accomplished by a

phase spatial light modulator or by a pure phase plate produced using the lithographic process. The electric field in the focal region can be written in the same form as Eq. (1); however, the two orthogonal components E_r and E_z are different and should be expressed as

$$E_r(r, z) = A \int_0^\alpha \sqrt{\cos(\theta)} \exp \left[i \cdot \pi \cdot \cos \left[\pi \cdot C \frac{\tan(\theta)}{\tan(\alpha)} \right] \right] \sin 2\theta P(\theta) l(\theta) J_1(kr \sin \theta) e^{ikz \cos \theta} d\theta \rightarrow (5)$$

$$E_z(r, z) = 2iA \int_0^\alpha \sqrt{\cos(\theta)} \exp \left[i \cdot \pi \cdot \cos \left[\pi \cdot C \frac{\tan(\theta)}{\tan(\alpha)} \right] \right] \sin^2 \theta P(\theta) l(\theta) J_0(kr \sin \theta) e^{ikz \cos \theta} d\theta \rightarrow (6)$$

The total intensity distribution in the focal region is proportional to the square modulus of Eq. (1), and the radial polarized component and longitudinal polarized component can be

calculated according to Eqs. (5) and (6) respectively. The $l(\theta)$ describes the radially polarized sinh-Gaussian beam, this function is given by

$$l(\theta) = \sinh^m \left(\frac{\sin(\theta)}{\omega_0} \right) \cdot \exp \left(-\frac{\sin^2(\theta)}{\omega_0^2} \right) \rightarrow (7)$$

Where ($m=0, 1, 2, \dots$) is the order of the hollow sinh-Gaussian beam. If $m=0$, the above equation is reduced to the fundamental Gaussian beam with beam waist of w_0 [22,23]. Obviously, for $m=0$, the beam governed by Eq. (7) is conventional Gaussian beam. However, a new kind of sinh-Gaussian beam is obtained when m is greater than 1.0. θ is determined by NA of objective lens and $0 \leq \theta \leq \arcsin(\text{NA}/n)$. Where, $n=1.0$ is the index of refraction of free space. Based on series, Eq. (7) can be considered as the sum of hollow Gaussian beam. Number of hollow

Gaussian beam and its characteristic are determined by parameter m and ω , simultaneously. If $m=0$, the above equation is reduced to the fundamental Gaussian beam with beam waist of w_0 . However, a new kind of sinh-Gaussian beam is obtained when m is greater than 1. It is noted that the amplitude distribution of hollow sinh-Gaussian beam is determined by ω_0 and m . $P(\theta)$ denotes the apodization function of the LG₁₁ beam, which is given as [24],

$$P(\theta) = \beta^2 \frac{\sin \theta}{\sin^2 \theta_{\max}} \exp \left[-\left(\beta \frac{\sin \theta}{\sin \theta_{\max}} \right)^2 \right] L_p^1 \left[2 \left(\beta \frac{\sin \theta}{\sin \theta_{\max}} \right)^2 \right] \rightarrow (8)$$

Here L_p is the generalized Laguerre polynomial and Truncation coefficient $\beta = R/w$ represents the ratio between R is the radius of the aperture and w is the waist of incident beam.

3. RESULTS AND DISCUSSION

The focusing characteristics of the higher order radially polarized sinh-Gaussian beam

with radial cosine phase wavefront are determined without losing validity. We carried out the integration of Eq. (1) numerically using parameters $\lambda = 1$, $\theta_{\max} = \arcsin(\text{NA})$, $\omega_0 = 0.500$, $\text{NA} = 0.9$ and $m = 2$. Here, for simplicity, we assume that both n and A have refractive indices of 1.

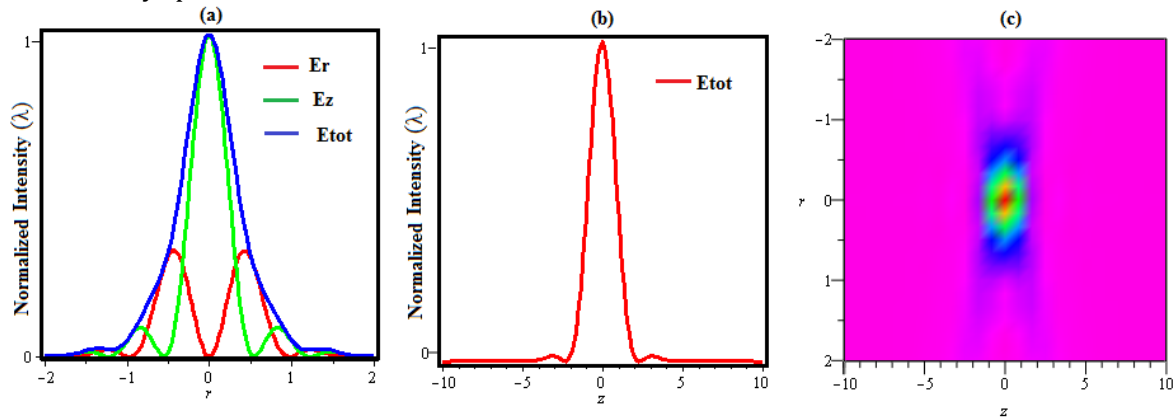


Figure 2 (a) 2D density distribution at $z = 0\lambda$ (b) Axial density at $r = 0\lambda$ (c) 3D density plot without wave front modulation with radial cosine phase

For all calculations, the length unit is normalized to λ and the energy density is normalized to unity. Without wavefront phase modulation, the focusing characteristics of a higher-order radially polarized sinh-Gaussian beam with a high NA lens system are investigated. Figure 2 (a-c) displays the intensity distribution of a higher-order radially

polarized sinh-Gaussian beam incident on the high NA lens. It is observed from the Fig. 2.a, we calculate the FWHM of the generated focal spot size to be 0.62λ and the focal depth to be 2.3λ , as shown in Fig. 2.b. Such a focal spot segment is useful for high-refractive-index particle trapping.

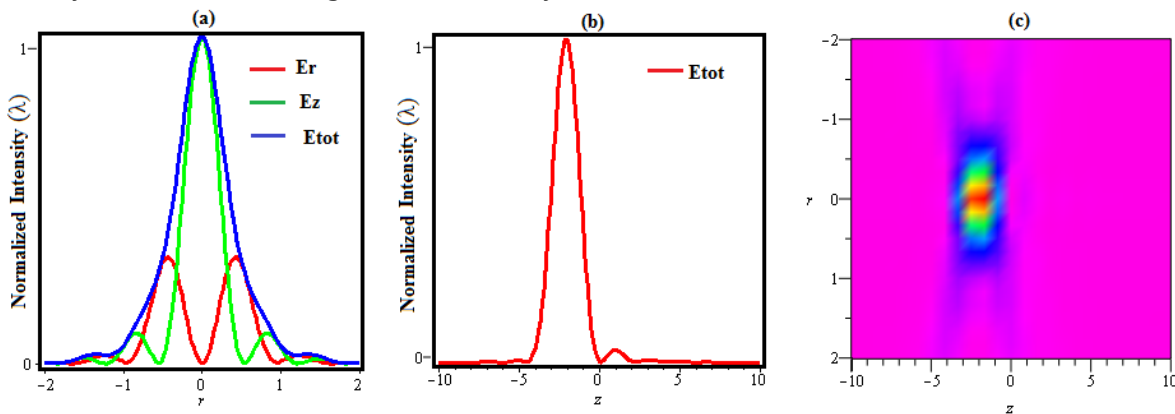


Fig.3.(a) 2D intensity distribution at $z = -2\lambda$ (b) On axial intensity at $r = 0\lambda$ (c) 3D intensity distribution in focal region for $C=1$ & $\beta=1$

The focal segment produced for frequency parameter values of $C=1$ is displayed in Fig. 3 (a-c). It can be seen from the Fig.3 (a) shows that the generated focal segment is a shifted focal spot size is 0.61λ . The maximum intensity location shifted to -2.2λ from Fig. 3 (b&c), and the focal depth 2.5λ .

However when we increased frequency parameter (C) values for $C=1.5$ the maximum intensity position shifted to -2.5λ is shown in fig.4. (c). From the Fig. 4.a, we measured the FWHM of the generated focal spot size is 0.95λ and focal depth 3.5λ which is shown in Fig. 4.b. We can see that the focal shift distance

increases on increasing phase parameter C almost linearly. If this focal peak is used to construct one optical trap, phase parameter C

may be employed to adjust trap position, can transport micro particles.

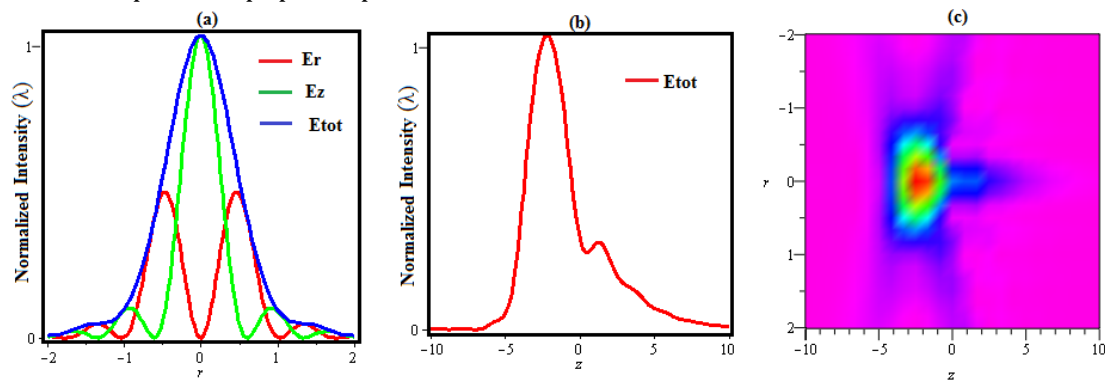


Fig 4 : (a) 2D intensity distribution at $z=-2\lambda$ (b) On axial intensity at $r=0\lambda$ (c) 3D intensity distribution in focal region for $C=1.5$ & $\beta=1$

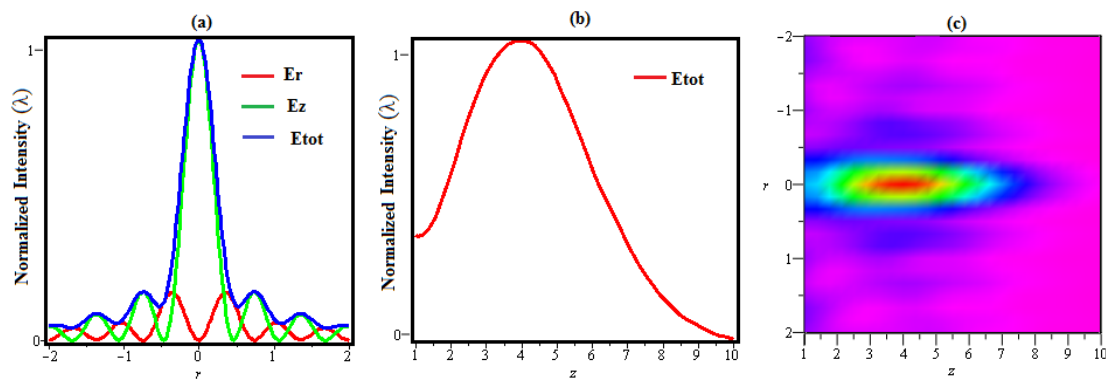


Fig 5: (a) 2D intensity distribution at $z=4\lambda$, (b) On axial intensity at $r=0\lambda$ (c) 3D intensity distribution in focal region for $C=2$ & $\beta=1$

The evolution of the high NA lens, the three-dimensional light intensity distribution for the values of the cosine parameter $C = 2$ is shown in Fig. 5. As the cosine parameter C is increased, the created focal spot in the focal region shifts away from the optical aperture along the optical axis, causing the focal shift phenomenon. Here, focal shift refers to a change in the position of maximum intensity. From this Figure, we measured the FWHM of the generated focal spot size of 0.42λ and focal depth of 6.5λ , and the maximum intensity position shifted to 4λ , which is shown in Fig. 5 (a-c). As parameter C is increased, the focus shift distance rises practically linearly. From the above focal pattern evolution process, we can see that for certain frequency parameters, C can alter considerably the intensity distribution in the focal region of a higher-order radially polarized sinh Gaussian beam, and many novel focal patterns can occur, which can be used to construct tunable optical traps.

Now the value of the truncation parameter β is changed to investigate its effect on focal pattern evolution. The intensity distributions for $\beta = 1.5$ and different C are illustrated in Fig. 6 (a-d). It can be seen from this figure that the truncation parameter affects very considerably the focal intensity distribution. On increasing the phase parameter $C=1$, the whole focal pattern shifts along the optical axis, with maximum intensity located at -4λ . Under the condition of $C = 1.5$, the whole focal pattern shifts along the optical axis near the optical aperture, and one intensity peak shrinks so that there is only one optical intensity maximum at -1λ . When C changes from 1 to 1.5, though, focal patterns differ very remarkably. In this sense, we call this optical barrier achieved by the focusing of the higher-order mode beam an optical cage. An optically dark spot has obvious applications for trapping particles with refractive indices lower than those of the surrounding medium and the single-beam blue-

detuned trapping of atoms in a low-intensity region. In the shifted optical cage suggested in this study, a particle in the center of the cage may receive a force with almost spherical symmetry. We predict that both the intensity symmetry and the polarization symmetry may

offer isotropic properties for trapping applications. Note that one can generate the optical cage by simply focusing a single higher-order radially polarized beam with appropriate truncation without any complicated interference instruments.

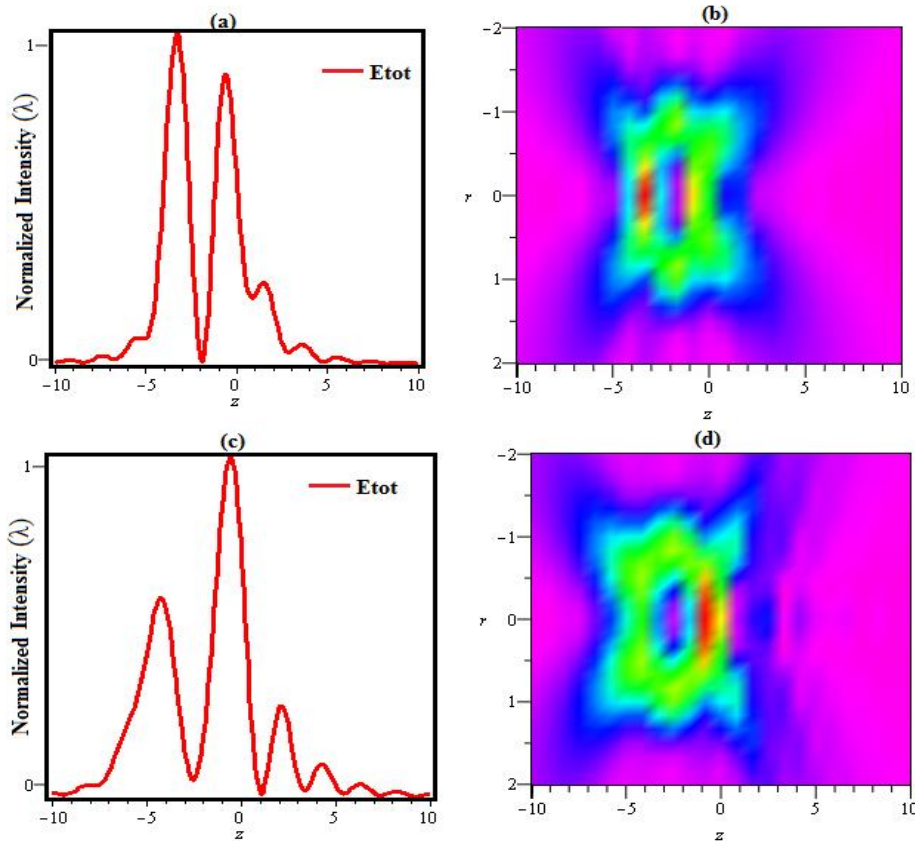


Fig 6: 2D & 3D Intensity distributions in focal region for NA = 0.9, $\beta = 1.5$, and (a & b) $C = 1$ (c & d) $C=1.5$ respectively

4. CONCLUSION

In conclusion, the focusing properties of a higher order radially polarized sinh-gaussian beam with radial cosine phase wavefront are extensively investigated based on the vector diffraction theory. The simulation results demonstrate that the frequency parameter (C) and truncation parameter (β) can be used to significantly modify the intensity distribution in the focal region of the higher order radially polarized sinh-gaussian beam. Focal spot can shift along optical axis on increasing C and β values, focal pattern changes are observed. Moreover, shifted optical cage focus pattern may appear in specific circumstances. The tunable focal shift can be used to construct controllable optical tweezers, atom guiding and trapping.

REFERENCES

- [1] Young worth, K.S. Brown, T.G, 2000. Focusing of high numerical aperture cylindrical vector beams. *Opt. Express* 7, 77-87.
- [2] Quabis,S, Dorn,R, Eberler, M., Glöckl, O., Leuchs, G., 2000. Focusing light to tighter spot. *Opt. Commun.* 179, 1-6.
- [3] Dorn,R, Quabis,S, Leuchs,G,2003. Sharper focus for a radially polarized light beam. *Phys. Rev. Lett.* 91, 233901
- [4] Nesterov, A.V., Niziev,V.G., 2000. Laser beams with axially symmetric polarization. *J. Phys. D* 33 1817.
- [5] Zhan,Q, 2004 Trapping metallic Rayleigh particles with radial polarization. *Opt. Express* 12, 3377-3382.

- [6] Kawauchi, H., Yonezawa, K., Kozawa, Y., Sato, S., 2007. Calculated the optical trapping forces on a microscopic particle in the ray optics regime for the case where a radially polarized laser beam. *Opt. Lett.* 32, 1839-1841
- [7] Nieminen, T.A., Heckenberg, N.R., Rubinsztein-Dunlop, H. 2008. Forces in optical tweezers with radially and azimuthally polarized trapping beams. *Opt. Lett.* 33, 122-124.
- [8] Yan, S., Yao, B., 2007. Radiation forces of a highly focused radially polarized beam on spherical particles. *Phys. Rev. A* 76, 053836.
- [9] Ahluwalia, B.P.S., Yuan, X.-C. Moh, K.J., Bu, J. 2007. Experimental transfer of torque induced by localized polarization of radially polarized vector beams to anisotropic microparticles, *Appl. Phys. Lett.* 91, 171102.
- [10] Chen, J., Ng, J., Liu, S., Lin, Z., 2009. Analytical calculation of axial optical force on a Rayleigh particle illuminated by Gaussian beams beyond the paraxial approximation. *Phys. Rev. E* 80, 026607.
- [11] Miyaji, G., Miyanaga, N., Tsubakimoto, K., Sueda, K., Ohbayashi, K., 2004. Intense longitudinal electric field from transverse electromagnetic waves. *Appl. Phys. Lett.* 84, 3855-3857.
- [12] Novotny, L. Beversluis, M., Youngworth, K.S., Brown, T., 2001. Longitudinal field modes probed by single molecules. *Phys. Rev. Lett.* 86, 5251.
- [13] Kozawa, Y., Sato, S. 2007. Sharper focal spot formed by higher-order radially polarized laser beams. *J. Opt. Soc. Am. A* 24(6), 1793-1798.
- [14] Kozawa, Y., Hibi, T., Sato, A., Horanai, H., Kurihara, M., Hashimoto, N., Yokoyama, H., Nemoto, T., Sato, S., 2011. Lateral resolution enhancement of laser scanning microscopy by a higher-order radially polarized mode beam. *Opt. Express* 19(17), 15947-15954.
- [15] Kozawa Y., Sato, S., 2012. Focusing of higher-order radially polarized Laguerre-Gaussian beam. *J. Opt. Soc. Am. A*, 29(11), 2439-2443.
- [16] Tian, B and Pu, J 2011. Tight focusing of a double-ring-shaped azimuthally polarized beam. *Opt. Lett.* 36(11) 2014-2016.
- [17] Moser, T., Glur, H., Romano, V., Pigeon, F., Parriaux, O., Ahmed, M.A., Graf, T. 2005. Polarization-selective grating mirrors used in the generation of radial polarization. *Appl. Phys. B* 80, 707-713.
- [18] Zhuang, Y., Zhang, Y., Ding, B., Suyama, T. 2011. Trapping Rayleigh particles using highly focused higher-order radially polarized beams. *Opt. Commun.* 284, 1734-1739.
- [19] Martines-Corral, M., Climent, V., 1996. Focal switch: a new effect in low-Fresnel-number systems. *Appl. Opt.* 35, 24-27.
- [20] Richards, B., Wolf, E., 1959. Electromagnetic diffraction in optical systems, II. Structure of the image field in an aplanatic system, *Proc. R. Soc. Lond. A Math. Phys. Sci.* 253 (1274) 358-379.
- [21] Gao, X., Li, J., Li, Z., Wang, J., Zhuang, S., 2010. Focusing of radially polarized beam with radial cosine phase wavefront. *Optik* 121, 1674-1680.
- [22] Jie Lin, Yuan Ma, Peng Jin, Graham Davies., Jiubin Tan, 2013. Longitudinal polarized focusing of radially polarized sinh-Gaussian beam. *Opt. Exp.* 21, 13193-13198.
- [23] Prabakaran, K., Karthik, V., Rajesh, K.B., Anbarasan, P.M., Aroulmoji, V., Mohamed Musthafa, A., 2020. Focal Hole Shifting of Azimuthally Polarized Sinh Gaussian Beam using Cosine Phase Filter, *Int. J. Adv. Sci. Eng.* 61476-1481
- [24] Prabakaran, K., Rajesh, K.B., Pillai, T.V.S., Jaroszewicz, Z., 2013. Focus shaping of tightly focused TEM₁₁ mode cylindrically polarized Laguerre Gaussian beam by diffractive optical element. *Optik* 124, 5039-5041.